Growth and Reactivity of Silver Clusters in Cyanide Solution

C. de Cointet, M. Mostafavi, J. Khatouri, and J. Belloni*

Laboratoire de Physico-Chimie des Rayonnements, Associé au CNRS, Bâtiment 350 Université Paris-Sud, 91405 Orsay, France

Received: October 28, 1996; In Final Form: February 27, 1997[⊗]

Pulse radiolysis was used to investigate the growth and reactivity dynamics of silver clusters in the presence of the cyanide ligands, Ag_{n,CN^-}, and of an electron acceptor/donor, the methyl viologen redox couple whose potential is $E°(MV^{2+}/MV^{\bullet+}) = -0.41\ V_{NHE}$. The absorbance of the $MV^{\bullet+}$ radical, produced by the same pulse as the silver atoms, is at first constant during an induction time delay, and then decays due to a catalytic electron transfer toward supercritical silver clusters. Correlated growth of the Ag_{n,CN^-} absorbance is also observed. Another process of reverse electron transfer from subcritical clusters to MV^{2+}, concomitant with the transfer from $MV^{\bullet+}$ to supercritical clusters, for the first time clearly appears to also occur in the kinetics. Through a numerical simulation model, including coalescence reactions between atoms or aggregates, catalytic electron transfer from $MV^{\bullet+}$ toward clusters above a critical size, and corrosion of subcritical aggregates by MV^{2+}, we derive the critical number n_c and the rate constants of the mechanism. The presence of CN^- causes a slowing of both the coalescence and electron transfer from $MV^{\bullet+}$ reactions. We conclude that $n_c = 5-6$ and hence that the reference redox potential in the presence of cyanide ligands corresponds to the couple $E°(Ag_{6-7}{}^{+},_{CN^-}/Ag_{6-7},_{CN^-}) \approx -0.4\ V_{NHE}$.

Introduction

Important advances in the thermodynamics of metal clusters in solution have been achieved through pulse radiolysis techniques. They allow the time-resolved observation of, first, the reduction of the ionic precursors into atoms, then of the progressive atom coalescence and of the cluster reactivity dependence on their nuclearity.[1−6] The most detailed mechanisms have been established for monovalent metal cations that are reducible by radiolytic species into atoms by a single monoelectronic step, such as Ag^+ with various ligands and surfactants,[1−11] $Au(CN)_2^-$,[12] or $CuCl_2^-$.[13,14]

Size-dependent properties of clusters are of crucial importance for their catalytic efficiency. Among catalyzed reactions, it has been shown that the electron-transfer reactions are indeed controlled by the nuclearity-dependent redox potential of the cluster.[15,16] The catalytic growth of silver clusters in the presence of a given electron donor is a specific example, quite similar to photographic development, where the donor potential constitutes a threshold that fixes a critical size for the transfer to be allowed.[1,4,15,16] The process is called autocatalytic insofar as the new atoms produced cause the growth of the catalyst, but in this particular case the concentration of active centers remains unchanged and it has no influence on the reaction rate.

However, up to now these time-resolved studies have concerned essentially monometallic clusters[3,5] or, less frequently, the early steps of mixed systems[1,17] even though it is well-known that alloyed bimetallic particles present a higher and more specific catalytic efficiency. The radiation-induced reduction of a mixed solution of two metal ions yields either composite clusters exhibiting a core−shell structure (with the more noble metal in the core) or intimately alloyed bimetallic clusters.[18] The result depends essentially on a possible concomitant electron transfer from the atoms of the less noble metal to the ions of the more noble metal. If the electron transfer is quite slow, the mixed association of atoms with ions of the second metal, followed by the reduction of these complexes, contributes to building alloyed clusters quite early on.[15] Some pulse radiolysis studies have already observed certain mixed transient species such as $(AgCd)^{2+}$ and $(AgCo)^{2+}$,[17] but since one of the metals was divalent, both ions could not be reduced at once.

The aim of this article and of the following[19] is to describe the time evolution of the pulse-induced reduction of a mixed system of two monovalent ions able to directly yield atoms and then to investigate the mechanism of their alloying during the coalescence and the reactivity of the bimetallic cluster with an electron donor. The bimetallic system selected is the couple $Au^I(CN)_2^-/Ag^I(CN)_2^-$, where both cations are monovalent and are complexed with the same ligand. Moreover, monometallic gold clusters prepared through reduction of $Au^I(CN)_2^-$ have been thoroughly studied,[12] and results concerning the early steps of $Ag^I(CN)_2^-$ reduction have been recently published.[8−10] This first part of the work will be devoted to the complete coalescence kinetics of silver atoms in the presence of the cyanide ligands and to the electron transfer from an electron donor to charged clusters as a prerequisite to the study of the mixed system.[19] A strong ligand such as cyanide is expected to have a marked influence on the metal cluster thermodynamics, as it does for the bulk metal.

Experimental Section

All reagents were pure chemicals: silver salt $KAg(CN)_2$ was from Comptoir Lyon Alemand Louyot, 2-propanol and acetone were from Prolabo, and methyl viologen chloride $MVCl_2$ was from Aldrich.

The pulse radiolysis facility (3 ns and 600 keV electron energy) and time-resolved optical detection have been described elsewhere.[20] The irradiation cell in Suprasil quartz allows optical absorption analysis (optical path 1 cm), penetration of the electron beam through a thin window, and circulation of the solution, which is removed after each pulse. However, due to side diffusion, the observation time range is limited to 40 s. Thus a Linac accelerator (1.5 μs pulse), delivering 4 MeV electrons, was also used in order to obtain the final absorption spectra, at longer times after the pulse, by conventional spectrophotometry in optical cells sealed under vacuum.

[⊗] Abstract published in *Advance ACS Abstracts,* April 1, 1997.

S1089-5647(96)03343-3 CCC: $14.00

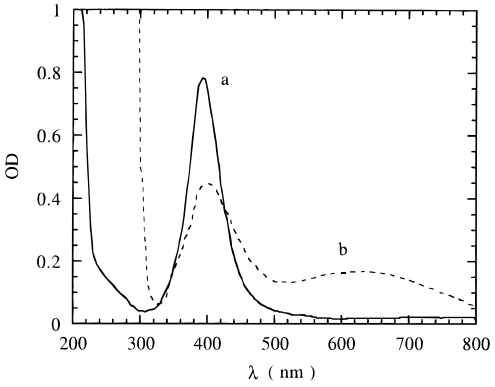

Figure 1. (a) Optical absorption spectrum of a 10^{-4} mol L^{-1} solution of $Ag(CN)_2^-$partially reduced by γ- irradiation. 2-Propanol: 0.2 mol L^{-1}. Optical length 1 cm. Dose = 0.160 kGy. (b) Optical absorption spectrum of a partially reduced solution of 5×10^{-4} mol L^{-1} $Ag(CN)_2^-$ in the presence of 5×10^{-4} mol L^{-1} MV^{2+} taken 5 min after the irradiation pulse. 2-Propanol: 0.2 mol L^{-1}. Optical length: 1 cm. Dose: 0.200 kGy.

Under irradiation aqueous solutions in the presence of 2-propanol are strong reducing media, due to the formation of hydrated electrons and of $(CH_3)_2C^{\bullet}OH$ radicals by alcohol scavenging of $OH^{\bullet}$ and $H^{\bullet}$ radicals. Due to the high sensitivity of the clusters to oxidation, all experiments were carried out in the strict absence of oxygen, removed by bubbling the solutions with an inert gas or under vacuum.

Results and Discussion

Silver Cyanide Solutions. The absorption spectrum of a γ-irradiated $KAg(CN)_2$ (10^{-4} mol L^{-1}) solution under vacuum does not change for doses higher than 400 Gy, which indicates total reduction. Then the spectrum remains unchanged despite the absence of any stabilizing agent in the solution (Figure 1a). The CN^- ligand of complexed ions adsorbed on clusters are efficient stabilizers of the colloid through electrostatic repulsion. The spectrum presents the characteristic plasmon band of silver clusters with a maximum at 395 nm. The extinction coefficient at 395 nm is $\epsilon_{395}(Ag_{n,CN^-}) = 21000$ L mol^{-1} cm^{-1}, somewhat higher than in sulfate solutions ($\epsilon_{395}(Ag_{n,SO_4^{2-}}) = 15\,000$ L mol^{-1} cm^{-1}).[21] The band is also narrower. Below 400 Gy, the increase of the absorbance is proportional to the dose. From the slope and from $\epsilon_{395}(Ag_{n,CN^-})$ one derives a G value of 2.3 atoms per 100 eV. The spectra readily vanish in the presence of air, indicating a fast oxidation of silver clusters by oxygen in cyanide solution, while the clusters are known to be stable when the counter anion is the sulfate.

After an electron pulse, the decay of the hydrated electron absorbance observed at 650 nm, in a solution containing 10^{-3} mol L^{-1} $KAg(CN)_2$ at pH $\approx$ 6, is pseudo-first-order. When plotted as a function of $Ag(CN)_2^-$ concentration, the first-order rate constant is linear and the bimolecular rate constant of reaction 1, under the above conditions, is close to the previously reported value $k_1 = 1.5 \times 10^9$ mol L^{-1} s^{-1}:

$$Ag^I(CN)_2^- + e_{aq}^- \rightarrow Ag^0(CN)_2^{2-} \qquad (1)$$

The reduction process is slower than in sulfate solutions ($k = 3.6 \times 10^{10}$ mol L^{-1} s^{-1} [21,23]) since the charge of uncomplexed Ag^+ is positive in the latter case, thus inducing a Coulombic attraction toward e_{aq}^-, while the charge is negative for $Ag(CN)_2^-$.

To check a possible role of the α-hydroxy alkyl radical in the reduction of $Ag(CN)_2^-$, e_{aq}^- were scavenged by adding acetone, which also produces this radical, so that it remains the only radical available. No Ag_n formation was observed, which means that $(CH_3)_2C^{\bullet}OH$ is unable to reduce any $Ag(CN)_2^-$ silver complex, and hence only hydrated electrons are involved in the primary reduction mechanism,[9] as for $Au(CN)_2^-$.[12] The G value found for the reduction yield without acetone under these pH conditions is the same as in γ-radiolysis and is slightly lower than the hydrated electron yield. The spectra of $Ag^0(CN)_2^{2-}$ and of the transient $Ag_2^{+}{}_{,CN^-}$ formed in the next step have been recently published.[8]

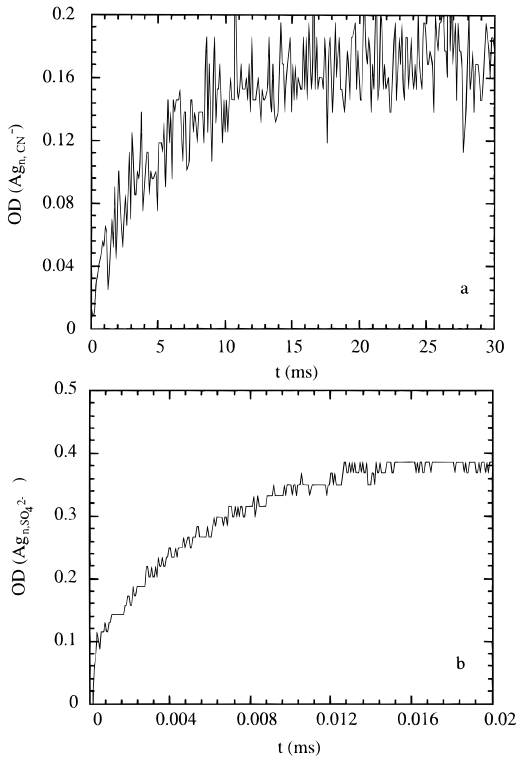

Figure 2. Comparison of the pulse radiolysis signals of the growth kinetics of silver clusters observed by their absorbance at 400 nm in the presence of (a) cyanide (2×10^{-3} mol L^{-1} $Ag(CN)_2^-$) or (b) sulfate (5×10^{-4} mol L^{-1} Ag_2SO_4). Deaerated solutions, pH 6, 0.2 mol L^{-1} 2-propanol.

In the time range of our measurements (up to 40 s), the 400 nm absorbance first increases, then tends to an asymptotic value (Figure 2a). The reducing species are readily exhausted during the first microsecond (reaction 1), and the radicals are no longer present in the medium over the millisecond range. The total amount of silver atoms therefore remains constant. Thus the absorbance increase at 400 nm in Figure 2a must be assigned to an increase in the extinction coefficient per silver atom in the clusters, induced by the coalescence as was already found for the system without CN^- ligands.[21] Also, as in the latter case, the coalescence rate constant k_d between two clusters may be supposed independent of the nuclearity n. Thus, the k_d value can be derived from results on the growth process kinetics. In fact, from the general model of growth kinetics[1,24] resulting from all coalescence reactions between two clusters of any size, it was stated that the kinetics should be superimposed, provided the total cluster concentration Σx_n is normalized relative to the initial concentration of atoms $x_0 = [Ag]_{t=0}$ as $\Sigma x_n/x_0$ and the time is expressed as t/τ with $\tau = 1/k_d x_0$.

The kinetics at 400 nm obtained in the present system (Figure 2a) is much slower than in the well-known Ag_2SO_4 system,[21] all other conditions being identical (Figure 2b). The plateau absorbance is also lower with cyanide, due to a smaller yield, and therefore the noise is more pronounced. According to the model[1,24] and assuming the same variation of the normalized value $\epsilon(n)/\epsilon(n\rightarrow\infty)$ in both media, the superimposition of the

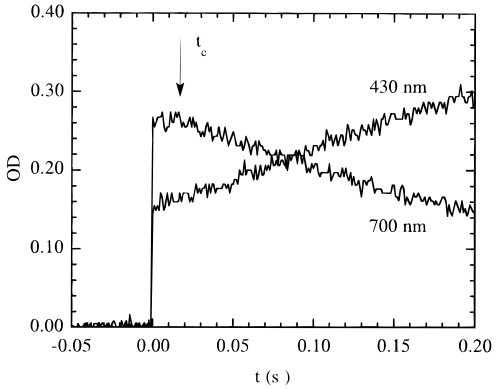

Figure 3. Single pulse correlated signals at $\lambda = 700$ nm and $\lambda = 430$ nm in a deaerated solution of 5×10^{-4} mol L^{-1} KAg $(CN)_2$, 5×10^{-4} mol L^{-1} MV^{2+}, and 0.2 mol L^{-1} 2-propanol. At 700 nm, decay of $MV^{\bullet+}$ after a time delay ($t_c \approx 15$ ms). At 430 nm, absorbance of both Ag_{n,CN^-} and $MV^{\bullet+}$.

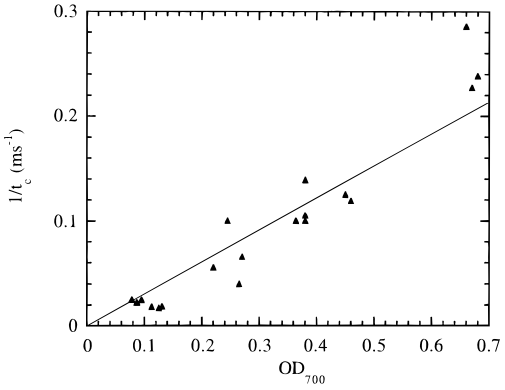

Figure 4. Dependence of the critical reciprocal time $(t_c)^{-1}$ on the initial absorbance at $\lambda = 700$ nm for variable doses per pulse. Same conditions as in Figure 3.

signals of Figure 2a,b should correspond to equal t/τ and $\Sigma x_n/x_0$:

$$\frac{k_d'}{k_d} = \frac{t}{t'}\frac{x_0}{x_0'} = \frac{t}{t'}\frac{\mathrm{OD}}{\epsilon}\frac{\epsilon'}{\mathrm{OD}'} \qquad (2)$$

where k_d, t, OD, and ϵ concern the cyanide solution and k_d', t', OD′, and ϵ' concern the sulfate solution. Indeed, signals of Figures 2a,b may be superimposed according to (2). The coalescence rate constant in sulfate medium being $k_d' = 2 \times 10^8$ L mol^{-1} s^{-1},[21] it follows from the signal comparison that $k_d = (6 \pm 2) \times 10^6$ L mol^{-1} s^{-1} in the presence of cyanide, i.e. more than 30 times slower than for the sulfate. From the coalescence rate constant value, the complete time evolution of the concentrations of all cluster nuclearities is derived.

Mixed Silver Cyanide and MV^{2+} Solutions. The redox potential of metal clusters in solution is known to increase with their nuclearity.[1,5,6,16] Therefore, in the presence of a redox probe S/S^- two cases are possible. First the aggregates may behave as an electron donor, for small n and $E°(Ag^+_{n,CN^-}/Ag_{n,CN^-}) < E°(S/S^-)$ (the positive charge of the clusters will symbolize its oxidized form although excess CN^- are adsorbed):

$$Ag_{n,CN^-} + S \rightarrow Ag^+_{n,CN^-} + S^- \qquad (3)$$

Second, the aggregates may behave as an electron acceptor for supercritical values of n and $E°(Ag^+_{n,CN^-}/Ag_{n,CN^-}) > E°(S/S^-)$:

$$Ag^+_{n,CN^-} + S^- \rightarrow Ag_{n,CN^-} + S \qquad (4)$$

Successively, both processes have to compete with the concomitant evolution of silver cluster coalescence. The critical aggregate Ag_{n_c,CN^-} corresponds to the thermodynamic threshold beyond which the electron transfer is reversed from reaction 3 to reaction 4. It corresponds to a critical size to which a redox potential $E°(Ag^+_{n,CN^-}/Ag_{n,CN^-})$ close to $E°(S/S^-)$ may therefore be assigned. The monoelectronic redox couple $MV^{2+}/MV^{\bullet+}$ was chosen because of the intense optical absorption band around 600 nm of $MV^{\bullet+}$ which behaves as the reference donor. In mixed solutions the hydrated electrons are scavenged partly by MV^{2+} and partly by $Ag(CN)_2^-$ in the range of 500 ns (Figure 3). The 2-propanol radicals are all scavenged by MV^{2+}. The evolution of silver cluster and electron donor signals is observed on different time scales, which correspond to successive steps of the process.

Time Range: 0.015 s < t < 0.15 s. Figure 3 presents the typical profiles of the time evolution of the absorbance at two wavelengths, $\lambda = 700$ nm and $\lambda = 430$ nm, obtained after the same pulse. $MV^{\bullet+}$ is observed at 700 nm where the spectrum is quite intense ($\epsilon_{700}(MV^{\bullet+}) = 3460$ L mol^{-1} cm^{-1}). In this time range the silver aggregates are small and hence do not exhibit any absorbance at this wavelength. At 430 nm, the $MV^{\bullet+}$ extinction coefficient is much smaller ($\epsilon_{430}(MV^{\bullet+}) \approx 1000$ L mol^{-1} cm^{-1}) than that of Ag_n. It appears that $MV^{\bullet+}$ (signal at 700 nm) is stable for ~15 ms under the conditions of Figure 3 before starting to decay. Correlatively, the 430 nm absorbance is first constant during the same period but then increases. As expected, the delay is induced by the time required for the clusters to grow enough such that their redox potential becomes higher than that of the reference donor, which imposes a threshold. The time delay t_c is much longer than the value measured when the reference is the radical of reduced sulfonato propyl viologen $SPV^{\bullet-}$ in the Ag_2SO_4/SPV system (~100 μs[1]), although other concentration conditions were identical and the reference couple potentials are very close: $E°(SPV/SPV^{\bullet-}) = E°(MV^{2+}/MV^{\bullet+}) = -0.41$ V_{NHE}.

The critical induction time, t_c, depends strongly on the initial atom concentration, fixed by the dose per pulse, on the coalescence rate constant and on the critical nuclearity selected by the donor potential. At variable doses and at a given ratio $[Ag(CN)_2^-]_0/[MV^{2+}]_0 = 1$, yielding a constant initial ratio of silver atoms and donor molecules according to the scavenging competition for e_{aq}^- and radicals, it is observed (Figure 4) that t_c^{-1} depends linearly in the range of uncertainty of measurements on the initial total absorbance at 700 nm (which is proportional to the dose), as has already been found in the kinetics model[1,24] and experimentally in the silver sulfate[1] or polyacrylate[4] systems.

Time Range: 0.15 s < t < 2 s. After the induction time, the $MV^{\bullet+}$ decay lasts for 1.5 s under the conditions of Figure 5, and in this interval the signal presents two successive steps, with a marked change in the slope at 0.2 and 1.5 s. The decay does not fit with a pseudo-first-order law except up to 0.15 s (Figure 5). The absorbance component after 1.5 s is due to large aggregates that are absent at shorter times. Their absorption spectrum, shifted toward higher wavelengths than for small clusters, is increasing, particularly beyond 10 s.

The slower decay after 0.2 s, which appears as a shoulder in the signal of Figure 5a did not exist in the Ag_2SO_4/SPV system. A possible reason could lie in the different charge of $SPV/SPV^{-\cdot}$ and $MV^{2+}/MV^{\bullet+}$ couples. Moreover, the perturbation of Ag_n,CN^- clusters by MV^{2+} must be very weak, as the ligand bound with CN^- is quite strong. This difference between both systems Ag^+ and $Ag(CN)_2^-$ is rather an indirect consequence of the slower coalescence process due to CN^-. Therefore, the

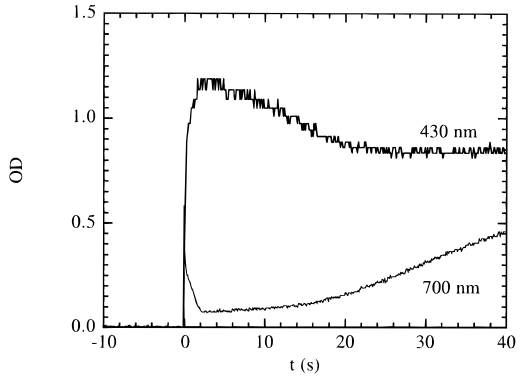

Figure 5. Correlated signals in the second range in solutions of $Ag(CN)_2^-/MV^{2+}$ (same conditions as in Figure 3) at (a) $\lambda = 700$ nm and (b) 430 nm. The signal at 700 nm is dominated by the $MV^{\bullet+}$ up to 2 s and then by the growth of large silver clusters. The intensity of their absorption spectrum at 430 nm also diminishes beyond 2 s.

shoulder is assigned to supplementary formation of $MV^{\bullet+}$ through the reversible reduction reaction of MV^{2+} by the subcritical silver clusters still present, which are thus corroded (reaction 7). This corrosion process is favored by the very slow coalescence, which during a longer time enhances the probability of encounters with MV^{2+}. A similar effect was found for the silver coalescence in Nafion membranes controlled by a very slow diffusion of atoms, thus favoring their oxidation by H_3O^+.[25] It is therefore necessary to include in the general mechanism the oxidation of these small aggregates (subcritical size $n < n_c$) with the rate constant k_{corr}:

$$\text{coalescence: } Ag_{m,CN^-} + Ag_{m,CN^-} \rightarrow Ag_{m+n,CN^-} \qquad k_d \quad (5)$$

$$\text{electron transfer: } Ag^+_{n>n_c,CN^-} + MV^{\bullet+} \rightarrow Ag_{n,CN^-} + MV^{2+} \qquad k_t \quad (6)$$

$$\text{corrosion: } Ag_{n<n_c,CN^-} + MV^{2+} \rightarrow Ag^+_{n,CN^-} + MV^{\bullet+} \qquad k_{corr} \quad (7)$$

Above n_c, reaction 6 is repeated as soon as a new silver ion adsorbs onto the supercritical cluster because the cluster redox potential is increasing, so that the cluster catalyzes its growth in an autocatalytic process.[1] Symmetrically, the reverse electron transfer from subcritical clusters to MV^{2+} (reaction 7) is even more favored when the redox potential decreases after the loss of an atom and is repeatedly autocatalyzed up to the complete dissolution of the cluster.[25] Reactions 6 and 7 do not represent an equilibrium because the nuclearities involved are not the same but are discriminated by n_c. In this mechanism the $MV^{2+}/MV^{\bullet+}$ couple indeed plays the role of an electron relay from the subcritical to the supercritical clusters. It is noteworthy that, although both electron transfers could be *a priori* expected (reactions 3, 4), they were not observed together until the present work, the required conditions being that the coalescence rate of (5) is slow enough and the corrosion rate of (7) is fast enough to affect reaction 6. The efficient oxidation of small clusters by MV^{2+} is also coherent with the high instability of these silver sols to oxygen in the presence of the CN^- ligand.

To determine the values of n_c, k_{corr}, and k_t, a numerical simulation model taking into account the value of k_d determined above and the cascades of successive coalescence (5), electron transfer (6), and corrosion reactions (7) was carried out. The experimental signal of the absorbance at 700 nm is compared in Figure 6 with the kinetics calculated using the adjusted values $n_c = 5$, $k_t = 5.3 \times 10^6$ L mol^{-1} s^{-1}, and three different values

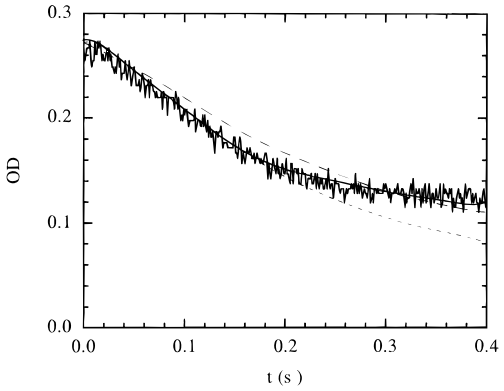

Figure 6. Comparison between an experimental signal (as in Figure 3 at 700 nm) and the numerical simulation: (- - -) $k_{corr} = 0$ L mol^{-1} s^{-1}; $k_d = 8 \times 10^6$ L mol^{-1} s^{-1}; $k_t = 4 \times 10^6$; $n_c = 5$; (— — —) $k_{corr} = 10^4$ L mol^{-1} s^{-1}; $k_d = 8 \times 10^6$ L mol^{-1} s^{-1}; $k_t = 4 \times 10^6$; $n_c = 5$; (—) $k_{corr} = 1.1 \times 10^2$ L mol^{-1} s^{-1}; $k_d = 8 \times 10^6$ L mol^{-1} s^{-1}; $k_t = 5.3 \times 10°$; $n_c = 5$.

of k_{corr}. If $k_{corr} = 0$, the deviation is important at $t > 0.2$ s. No adjustment of n_c and k_t alone could account for the observed features of the signals, particularly for the shoulder described above. In this example the best fit is obtained for $k_{corr} = 1.1 \times 10^2$ L mol^{-1} s^{-1}.

The adjusted parameters are valid for the experimental signals obtained under different dose-per-pulse conditions with the following uncertainties:

$$n_c = 5 \text{ or } 6; \quad k_d = (6 \pm 2) \times 10^6 \text{ L mol}^{-1} \text{ s}^{-1}; \quad k_t = (5.3 \pm 0.1) \times 10^6 \text{ L mol}^{-1} \text{ s}^{-1}; \quad k_{corr} = (1.0 \pm 0.2) \times 10^2 \text{ L mol}^{-1} \text{ s}^{-1} \quad (8)$$

It has been noted above that the expected linear variation of t_c^{-1} *vs* the initial atom concentration was indeed observed (Figure 4). In fact, at low atom concentration the observed t_c is somewhat longer than the linear variation precisely because the corrosion of subcritical clusters is comparatively more important.

The value of the critical size $n_c = 5-6$ corresponds to the redox potential of the cluster containing one more silver cation *i.e.* of the couple $E°(Ag_{6-7}^+,_{CN^-}/Ag_{6-7,CN^-}) \approx -0.4$ V_{NHE}. This value compared with $E°(Ag_5^+,_{SO_4^{2-}}/Ag_{5,SO_4^{2-}}) \approx -0.4$ V_{NHE} obtained in the sulfate environment means that at the same nuclearity the small cluster redox potential in the presence of the cyanide ligand is lower than for clusters without a ligand. This result differs from the effect of the polyacrylate surfactant, which also slowed down the coalescence rate constant but had no effect on the critical size.[5] Note that the presence of the cyanide ligand induces also a decrease compared to the sulfate medium on the electrochemical potential of the bulk silver electrode $E°(Ag(CN)_2^-/Ag_{metal}) = -0.395$ V_{NHE}[26] and on the redox potential of the single silver atom $E°(Ag_1^+,_{CN^-}/Ag_{1,CN^-}) = -2.6$ V_{NHE}.[7] The lengthening of the critical time in the presence of CN^- compared to SO_4^{2-} results mostly from a slower coalescence process and to a lesser extent from a higher critical nuclearity required to reach the potential threshold imposed by the donor.

Time Range: 2 s < t < 40 s. Beyond 2 s the decay at 700 nm is followed by a strong increase correlated with a decay at 430 nm (Figure 5). The new absorbance component at 700 nm is specific to large silver aggregates absent at short time. They are more and more abundant in the distribution, partly because of the increasing coalescence in the absence of any

surfactant, but mostly because of the important development by $MV^{\bullet+}$ of the low initial concentration of catalytic germs (increase at 430 nm in Figure 3). Simultaneously, the silver plasmon band, characteristic of small aggregates, decreases: this phenomenon is followed at 430 nm, where Ag_{n,CN^-} is the sole absorber after $MV^{\bullet+}$ has disappeared ($t > 2$ s) (Figure 5b). Note that after 2 s the clusters present are no longer corroded by excess MV^{2+} because only supercritical clusters have survived.

A few minutes after irradiation, two bands appear in the final optical spectrum of the irradiated solution, one at 400 nm and another less intense around 600 nm (Figure 1b). This shape is different from that obtained without the viologen and is indeed characteristic of large developed silver aggregates, resulting from the catalytic growth through electron transfer from $MV^{\bullet+}$. These clusters with an absorbance in the red were already observed in the Ag_2SO_4/SPV system and well identified by electron microscopy.[1]

Conclusion

The pulse radiolysis method has allowed the kinetics study of the ion reduction and the cluster growth in silver cyanide solutions as a preliminary study to the investigation of mixed $Ag(CN)_2^-/Au(CN)_2^-$ solutions.[19] From the time-resolved observation of the reaction of an electron donor acting as a developer of supercritical silver aggregates and of the catalytic growth of these centers, it appears that reduction by an electron in the presence of cyanide occurs at larger critical size of the aggregate than with sulfate for a similar redox probe.

The CN^- environment slows down the kinetics of both the coalescence and the electron transfer and lowers the cluster redox potential scale. Both phenomena decrease the stability of nascent metal clusters toward oxidation. This study provides the first observation of the growth of supercritical clusters together with the corrosion of the subcritical ones by the oxidized form of the donor, the latter process being indeed favored by the slow coalescence. The numerical simulation of the donor decay also allows the evaluation of the oxidation rate constant of the subcritical clusters. These results are of high interest for yielding a quantitative evaluation of the role of ligands on the cluster thermodynamics.

Acknowledgment. We are indebted to our colleague Dr. P. Pernot from the laboratory for his helpful collaboration in the computer simulation and to Dr. V. Favaudon from the Curie Institute, Orsay, for the access to the Linac facility. We are grateful to AGFA-GEVAERT Company for financial support.

References and Notes

(1) Mostafavi, M.; Marignier, J. L.; Amblard, J.; Belloni, J. *Radiat. Phys. Chem.* **1989**, *34*, 605; *Z. Phys. D*: *At., Mol. Clusters* **1989**, *12*, 31.
(2) Henglein, A. *Chem. Rev.* **1989**, *89*, 1861.
(3) Henglein, A. *J. Phys. Chem.* **1993**, *97*, 5457.
(4) Mostafavi, M.; Delcourt, M. O.; Belloni, J. *J. Imaging Sci. Technol.* **1994**, *38*, 54.
(5) Belloni, J.; Amblard, J.; Marignier, J. L. In *Clusters of Atoms and Molecules;* Graduate Texts in Contemporary Physics; Haberland, H., Ed.; Springer-Verlag: Berlin, **1994**; Vol. II, p 290.
(6) Belloni, J. *Curr. Opin. Colloid Surf. Sci.* **1996,** *1*, 184.
(7) Remita, S.; Archirel, P.; Mostafavi, M. *J. Phys. Chem.* **1995**, *99*, 13198.
(8) Remita, S.; Mostafavi, M.; Delcourt, M. O. *J. Phys. Chem.* **1996**, *100*, 10187.
(9) Texier, I.; Mostafavi, M. *Radiat. Phys. Chem.* **1997**, in press.
(10) Mostafavi, M.; Remita, S.; Delcourt, M. O.; Belloni, J. *J. Chim. Phys.* **1996**, *93*, 1828.
(11) Texier, I.; Remita, S.; Archirel, P.; Mostafavi, M. *J. Phys. Chem.* **1996**, *100*, 12472.
(12) Mosseri, S.; Henglein A.; Janata, E. *J. Phys. Chem.* **1989**, *93*, 6791.
(13) Ershov, B. G.; Sukhov N. L. *Radiat. Phys. Chem.* **1990**, *36*, 93. Ershov, B. G.; Sukhov, N. L.; Troitski D. I. *Radiat. Phys. Chem.* **1992**, *39*, 123.
(14) Khatouri, J.; Mostafavi, M.; Amblard, J.; Belloni, J. *Chem. Phys. Lett.* **1992,** *191*, 351; *Z. Phys. D: At. Mol. Clusters* **1993**, *26*, 82.
(15) Belloni, J.; Delcourt, M. O.; Marignier, J. L.; Amblard, J. in *Radiation Chemistry*; Hedwig, P., Nyikos, L., Schiller, R., Eds.; Akad. Kiado: Budapest, Tihany, 1987; p 89.
(16) Khatouri, J.; Mostafavi, M.; Belloni, J. In *Photochemisty and Radiation Chemistry: Complementary Methods for the Study of Electron Transfer*; Wishart, J., Nocera, D., Eds.; ACS: Washington, DC, 1997.
(17) Ershov, B. G.; Janata, E.; Henglein A. *J. Phys. Chem.* **1994,** *98*, 7619 and 10891.
(18) Marignier, J. L.; Belloni, J.; Delcourt, M. O.; Chevalier J. P. *Nature* **1985**, *317*, 344.
(19) de Cointet, C.; Khatouri, J.; Mostafavi M.; Belloni, J. *J. Phys. Chem. B* **1997**, *101*, 3517.
(20) Belloni, J.; Billiau, F.; Cordier, P.; Delaire, J. A.; Delcourt, M. O. *J. Phys. Chem.* **1978**, *82*, 532.
(21) Henglein, A.; Tausch-Treml, R. *J. Colloid Interface Sci.* **1981**, *80*, 84.
(22) Anbar, M.; Hart, E. J. *J. Phys. Chem.* **1965,** *69*, 973.
(23) Anbar, M.; Bambenek, M.; Ross, A. B. *NBS Ref. Data Ser.* **1973,** *43*.
(24) Khatouri, J.; Mostafavi, M.; Amblard, J.; Ridard, J.; Belloni, J. *Z. Phys. D: At, Mol. Clusters* **1995**, *34*, 47 and 57.
(25) Platzer, O.; Amblard, J.; Marignier, J. L.; Belloni J. *J. Phys. Chem.* **1992**, *96*, 2334. Amblard, J.; Platzer, O.; Ridard, J.; Belloni J. *J. Phys. Chem.* **1992**, *96*, 2341.
(26) Gauguin, R. *J. Chim.Phys.* **1945**, *42*, 28.